HHS Public Access

Author manuscript

J Immunol. Author manuscript; available in PMC 2017 August 23.

Published in final edited form as:

J Immunol. 2017 January 01; 198(1): 257–269. doi:10.4049/jimmunol.1601200.

Temporal Expression of Bim Limits the Development of Agonist-Selected Thymocytes and Skews Their TCRβ Repertoire

Kun-Po Li[*,†], **Anke Fahnrich**[‡], **Eron Roy**[*,†], **Carla M. Cuda**[§], **H. Leighton Grimes**[*,†], **Harris R. Perlman**[§], **Kathrin Kalies**[‡], and **David A. Hildeman**[*,†]

[*]Division of Immunobiology, Cincinnati Children's Hospital Medical Center, Cincinnati, OH 45229

[†]Department of Pediatrics, University of Cincinnati, Cincinnati, OH 45257

[‡]Institute for Anatomy, University of Lübeck, 23538 Lübeck, Germany

[§]Rheumatology Division, Department of Medicine, Feinberg School of Medicine, Northwestern University, Chicago, IL 60611

Abstract

CD8αα TCRαβ$^+$ intestinal intraepithelial lymphocytes play a critical role in promoting intestinal homeostasis, although mechanisms controlling their development and peripheral homeostasis remain unclear. In this study, we examined the spatiotemporal role of Bim in the thymic selection of CD8αα precursors and the fate of these cells in the periphery. We found that T cell–specific expression of Bim during early/cortical, but not late/medullary, thymic development controls the agonist selection of CD8αα precursors and limits their private TCRβ repertoire. During this process, agonist-selected double-positive cells lose CD4/8 coreceptor expression and masquerade as double-negative (DN) TCRαβ^{hi} thymocytes. Although these DN thymocytes fail to re-express coreceptors after OP9-DL1 culture, they eventually mature and accumulate in the spleen where TCR and IL-15/STAT5 signaling promotes their conversion to CD8αα cells and their expression of gut-homing receptors. Adoptive transfer of splenic DN cells gives rise to CD8αα cells in the gut, establishing their precursor relationship in vivo. Interestingly, Bim does not restrict the IL-15–driven maturation of CD8αα cells that is critical for intestinal homeostasis. Thus, we found a temporal and tissue-specific role for Bim in limiting thymic agonist selection of CD8αα precursors and their TCRβ repertoire, but not in the maintenance of CD8αα intraepithelial lymphocytes in the intestine.

The intestinal epithelium continuously contacts food Ags and intestinal flora and relies on a complex network of intestinal immune cells that control immune homeostasis in the gut. Besides CD4$^+$ regulatory T cells (Tregs) and TCRgδ$^+$ cells, a high level of

Address correspondence and reprint requests to Dr. David A. Hildeman, Department of Pediatrics, Division of Immunobiology MLC 7038, Cincinnati Children's Hospital Medical Center, 3333 Burnet Avenue, Cincinnati, OH 45229. David.Hildeman@cchmc.org.

ORCIDs: 0000-0002-8872-3814 (K.-P.L.); 0000-0002-7181-7929 (E.R.); 0000-0001-8162-6758 (H.L.G.); 0000-0003-4174-608X (H.R.P.); 0000-0002-8929-4249 (K.K.); 0000-0002-0421-8483 (D.A.H.).

The online version of this article contains supplemental material.

Disclosures

The authors have no financial conflicts of interest.

TCRαβ$^+$CD8αα$^+$ and TCRαβ$^+$CD4$^-$CD8$^-$ double-negative (DN) T cells reside in the intestinal intraepithelial lymphocyte (iIEL) compartment. Both DN and CD8αα iIELs play an immune regulatory role in the intestine, secreting immune-suppressive cytokines to prevent inflammatory bowel diseases (1–4). With regard to TCRαβ CD8αα iIELs, there has been some controversy surrounding their development. Although earlier work suggested that this population is extrathymically derived (5, 6), more recent studies suggest that most TCRαβ CD8αα iIELs in euthymic mice are derived from thymic precursor cells, which are selected by the agonist peptide/MHC complex stimulating TCRs with a strong affinity (7–12). This “agonist selection” developmental model of the CD8αα iIELs and DN T cells was further strengthened by recent experiments using TCR-transgenic mice in which the TCRs were derived from CD8αα iIELs, in that the mice bearing these iIEL-derived self-reactive TCRs had an abundance of CD8αα iIELs and DN T cells (13–15). These studies showed that the TCRs favoring DN and CD8αα T cell differentiation may promiscuously interact with multiple ligands, including MHC class I, MHC class II (MHC II), or nonclassic MHC ligands (14, 15). During thymic development, a considerable portion of thymocytes with these TCRs undergo apoptosis. How the self-reactive thymic precursors of CD8αα T and DN T cells survive negative selection-associated apoptosis and develop into mature iIELs are not well understood mechanistically.

T cells with strong avidity for self-antigens are limited in the thymus, whereas a broad T cell repertoire restricted to self-MHC molecules is maintained by the mechanisms of central tolerance. After TCR V(D)J rearrangement, positive selection takes place in thymic cortex and promotes the survival of CD4$^+$CD8$^+$ double-positive (DP) thymocytes whose TCRαβ has at least a basal affinity for self-antigen peptide/MHC complexes. Positively selected thymocytes then undergo two waves of thymic negative selection. One wave occurs in response to ubiquitous self-antigen (UbA) and endogenous viral superantigen (SAg) in the thymic cortex or corticomedullary junction (16). A second wave occurs when CCR7 signals direct thymocytes into thymic medulla and responses to tissue-restricted self-antigen (TRA) driven by medullary thymic epithelial cells and dendritic cells in an Aire-dependent manner (16). Those having too strong affinity are eliminated during negative selection (17).

The negative selection process has been reported to be mediated by the BH3-only Bcl-2 family member Bim, as Bim$^{-/-}$ mice are resistant to thymic negative selection in five independent models (18). Paradoxically, Bim$^{-/-}$ mice do not have an increase in DP (CD4$^+$CD8$^+$) thymocytes as would be expected if thymic negative selection were impaired (19). Additionally, other groups have failed to find a substantial role for Bim in other models of thymic negative selection, including endogenous SAg- or UbA-induced negative selection, which are thought to better represent physiologic negative selection (20, 21). One possibility is that other proapoptotic factors, such as Puma, may serve redundant roles with Bim to fully promote negative selection (22). Another non–mutually exclusive possibility is that Bim plays a more important role in a certain type of thymocytes undergoing negative selection, such as those responding to TRA (23, 24). However, many of these studies only focused on the negative selection of conventional T cells. The spatial and temporal role of Bim in agonist selection remains unclear.

Several groups characterized the mice overexpressing Bcl-2, or those lacking expression of Bim, and found an accumulation of DN4-like ($CD4^-CD8^-CD44^-CD25^-$) thymocytes that appear to have increased surface expression of TCRβ (20, 24–26). It is proposed that TCR^+DN thymocytes are the thymic precursors of CD8αα iIELs based on in vitro culture and adoptive transfer experiments (11, 25, 27). Consistently, $Bim^{-/-}$ mice also have significantly increased accumulation of $TCR\alpha\beta^+$ CD8αα iIELs (13). These data suggest that Bim may control the development of CD8αα iIELs during the thymic stage. However, the details of CD8αα iIEL development have not been carefully characterized.

CD8αα T cells are maintained in the intestinal epithelium by IL-15 (28, 29). It was reported that intestinal IL-15Rα trans-presentation of IL-15 locally promotes development and survival of CD8αα iIELs (30, 31). IL-15 also promotes peripheral T lymphocyte survival by increasing their expression of Bcl-2, which antagonizes the effects of proapoptotic Bim (21, 30, 32, 33). Although prior reports suggested that IL-15 similarly antagonized Bim in CD8αα iIELs (34, 35), its role in vivo has not been fully examined.

In this study, we examined the development and homeostasis of DN and CD8αα T cells using mice with temporal- and tissue-specific expression of Cre to drive deletion of Bim. We found that TCR^+DN thymocytes and their peripheral descendants were limited by Bim at the early DP stage. We also found that Bim critically shapes the TCRβ repertoire of DN T cells, but not of conventional T cells. Furthermore, we found that splenic DN T cells could give rise to CD8αα cells in the gut, and IL-15 acting via Stat5 synergized with TCR signaling to promote this process. Collectively, these data show the temporal- and tissue-specific role of Bim in limiting the agonist selection of $TCR\alpha\beta^+$DN thymocytes, the precursors of peripheral DN and CD8αα T cells, and they uncover interactions between Bim and IL-15 that control the postthymic development and homeostasis of DN and CD8αα T cells.

Materials and Methods

Mice

C57BL/6 mice were purchased from Taconic Farms (Germantown, NY). $Bim^{-/-}$ mice were a gift from P. Bouillet and A. Strasser (Walter and Eliza Hall Institute, Melbourne, VIC, Australia) and have been backcrossed to C57BL/6 mice for at least 20 generations. $Bax^{f/f}Bak^{-/-}$ mice were a gift from S. Korsmeyer (Harvard Medical School, Boston, MA) and were crossed to dLckCre or LckCre mice obtained from The Jackson Laboratory (Bar Harbor, ME). IL-15–deficient mice on a C57BL/6 background were purchased from Taconic Farms and were bred with $Bim^{-/-}$ mice in our facility. Generation of $dLckCre^+Bim^{f/f}$ mice was described (36). $Bim^{f/f}$ mice were also crossed to $CD4Cre^+$ mice obtained from The Jackson Laboratory. STAT5a/$b^{f/f}$ mice were a gift of L. Hennighausen (National Institutes of Health, Bethesda, MD) and were crossed to C57BL/6 mice, and then crossed to $dLckCre^+Bim^{f/f}$ mice as previously described (32). B6. SJL-*Ptprc*^{a}*Pepc*^{b}/BoyCrCrl (BoyJ) mice were purchased from Charles River Laboratories (Wilmington, MA). All mice were used between 5 and 10 wk of age. Animals were housed under specific pathogen-free conditions in the Division of Veterinary Services (Children's Hospital Medical Center, Cincinnati, OH), and experimental procedures were reviewed and approved by the

Institutional Animal Care and Use Committee at the Cincinnati Children's Hospital Research Foundation.

Cell processes and flow cytometry

Thymi, lymph nodes, or spleens from individual mice were harvested and crushed through a 100-μm mesh cup to generate single-cell suspensions. IELs isolation was performed by following a modified protocol (37). Briefly, the small intestine was cut off and washed with $Ca^{2+}Mg^{2+}$-free HBSS for removing feces and mucus. After removing Peyer's patches, the small intestine was cut in pieces and shaken in $Ca^{2+}Mg^{2+}$-free HBSS supplemented with 5% FBS, 2 mM EDTA, and 1 mM DTT (Sigma-Aldrich, St. Louis, MO). After incubation for 15 min at 37°C, the IELs in the supernatant were further purified with Percoll (GE Healthcare, Little Chalfont, U.K.) gradient. The single-cell suspension was further analyzed by flow cytometry. Two million or more cells were stained with Abs against CD4, CD8α, TCRβ, TCR-Vα2, TCR-Vα11 (BD Biosciences, San Diego, CA), CCR7, CD5, CD19, CD24, CD25, CD44, CD45.2, TCR-Vα3.2, NK1.1, MHC II (I-A/I-E) (eBioscience, San Diego, CA), CD8β, CD45.1, TCR-Vα8.3, $\alpha_4\beta_7$ (LPAM-1), CCR9 (BioLegend, San Diego, CA), Bim, or Stat5 (Cell Signaling Technology, Beverly, MA). Intracellular stains were performed using 2% paraformaldehyde for fixation and 0.03% saponin for staining. For detection of Bim, secondary anti-rabbit IgG Ab was used (Life Technologies, Carlsbad, CA). A minimum of 200,000 events was acquired on a BD LSR II flow cytometer and analyzed by FACSDiva software (BD Biosciences).

Cell culture

OP9-DL1 cells were cultured as previously described (38). Sorted DN4 or DN1-3 thymocytes from wild-type (WT) or $Bim^{-/-}$ mice were cocultured with OP9-DL1 cells in a 1:5 ratio and supplied with 1 ng/ml IL-7 (R&D Systems, Minneapolis, MN) for 1–4 d. In DN T cell differentiation culture, splenic DN T cells ($CD4^{-}CD8\alpha^{-}TCR\beta^{+}$) were sorted out and cultured for 24–48 h with 20 ng/ml exogenous rIL-2 supplement (R&D Systems). In some experiments, the DN T cells were stimulated with plate-bound anti-CD3/CD28 Ab (5 μg/ml; R&D Systems), IL-15 (20 ng/ml; R&D Systems), or both.

Cell sorting and adoptive transfer

Indicated splenocyte or thymocyte populations were sorted on MoFlo XDP (Beckman Coulter, Brea, CA) with the assistance of the Research Flow Cytometry Core at Cincinnati Children's Hospital Medical Center. In adoptive transfer experiments, DN T cells were sorted on $CD4^{-}CD8\alpha^{-}$ $CD19^{-}NK1.1^{-}MHC\ II^{-}$ cells. One million DN T cells were i.v. adoptively transferred to each BoyJ recipient. After 7 d, the lymphocytes in spleens, mesenteric lymph nodes, and small intestinal epithelium were analyzed by flow cytometry.

Analysis of CDR3 sequence of TCRβ-chains

RNA from sorted $CD4^{+}$ T, $CD8^{+}$ T, or DN T cells was isolated with an innuPREP RNA Mini Kit (Analytik Jena, Hildesheim, Germany). TCRβ-chain sequences were amplified in a two-step reaction according to the manufacturer's protocol (iRepertoire, patent 7999092). The first reverse transcription was performed with a OneStep RT-PCR kit (Qiagen, Hilden,

Germany), and the second round of PCR was performed with nested primers, sequencing adaptors A and B following paired-end sequencing (Illumina). PCR products were purified using a QIAquick gel extraction kit (Qiagen) after gel electrophoresis. About 2 million sequencing reads were obtained from each sample of the TCRβ library, sequenced with the Illumina 300-cycle MiSeq reagent kit v2 (150 paired-end read). CDR3 identification, clonotype clusterization, and correction of PCR and sequencing errors were performed using MiTCR software (39) according to the IMGT nomenclature (40). To avoid unpredictable PCR and sequencing errors, the default parameters ("eliminate these errors") was used. Additionally, to avoid artificial diversity due to PCR errors, low abundance sequence variants that comprise 4% of all sequencing reads were removed as described (41). For normalizing data from different samples to a common scale, TCR sequences were subsampled randomly to the lowest number of sequences produced from any sample (n = 1000). Further data analysis (principal component analysis [PCA] and CDR3 length) were performed using R programming language, including the tcR package (42).

Results

TCR expressing CD4$^-$CD8$^-$ CD25$^-$CD44$^-$ DN thymocytes accumulate in Bim$^{-/-}$ mice

Initial work indicated a role for Bim in the elimination of autoreactive thymocytes (18), although others have suggested a minor role for Bim in thymocyte negative selection (20, 21). Furthermore, Bim$^{-/-}$ mice have an accumulation of TCRβ$^+$DN4 thymocytes, although these cells have not been fully characterized (26). Hence, we assessed thymocytes in Bim$^{-/-}$ mice and found there was a significant increase in the frequency and the total number of DN (CD4$^-$CD8$^-$) thymocytes in Bim$^{-/-}$ mice (Fig. 1A). Furthermore, most of these cells (>93%) also lacked expression of CD44 or CD25, placing them in the DN4 compartment (Fig. 1A). Strikingly, nearly all of these DN4-like thymocytes in Bim$^{-/-}$ mice expressed high levels of cell surface TCRβ-chain (Fig. 1B). Staining these DN4-like thymocytes with a combination of TCR-Vα Abs (Vα2, Vα3.2, Vα8.3, and Vα11), in lieu of a pan-TCRα Ab, further showed that the TCRβ-chains were associated with cell surface TCRα-chains. In fact, the frequencies of TCRα$^+$ DN4-like thymocytes from Bim$^{-/-}$ mice were similar to the frequencies of TCRα$^+$ CD4 single-positive (SP) or CD8SP cells in either WT or Bim$^{-/-}$ mice (Fig. 1C). Thus, the vast majority of DN4-like cells in Bim$^{-/-}$ mice do not display characteristics of normal DN4 cells from WT mice, especially with regard to cell surface αβTCR expression.

TCR$^+$DN cell accumulation is thymocyte intrinsic and Bim-Bax/Bak–dependent

Next, we took advantage of LckCre$^+$Bax$^{f/f}$Bak$^{-/-}$ mice, as Bax and Bak are required for Bim-driven death (33). These mice have a global deletion of Bak, combined with a T cell-specific loss of Bax due to the Lck promoter-driven Cre recombinase as early as DN1 stage (43). Similar to Bim$^{-/-}$ mice, LckCre$^+$ Bax$^{f/f}$Bak$^{-/-}$ mice also had a significant accumulation of TCRβ$^+$DN thymocytes (Supplemental Fig. 1A). Collectively, these data show that the accumulation of TCRβ$^+$DN thymocytes is limited by thymocyte-intrinsic apoptosis driven by Bim/Bax/Bak.

CD4 promoter–driven deletion of Bim results in accumulation of TCR$^+$DN thymocytes

One explanation for these data is that these DN4-like cells were cells that had escaped negative selection in Bim$^{-/-}$ mice but had down-regulated CD4 and CD8 coreceptor expression (25, 26, 44). To test this, we generated mice in which Bim was selectively deleted in DP thymocytes by mating CD4Cre mice to Bim$^{f/f}$ mice. The rationale is that if these TCR$^+$DN cells were previously DP cells, then deletion of Bim only after expression of CD4 (using CD4Cre) should result in an increase in TCR$^+$DN cells. Conversely, if these TCR$^+$DN cells are not increased in CD4Cre$^+$Bim$^{f/f}$ mice, then these cells arise prior to the DP stage. Notably, assessment of thymocytes in CD4Cre$^+$Bim$^{f/f}$ mice revealed an increase in DN thymocytes, with most being CD44$^-$ CD25$^-$ and expressing surface TCRβ (Fig. 2A, 2B). Similar to Bim$^{-/-}$ mice, a significant fraction of DN4 thymocytes in CD4Cre$^+$ Bim$^{f/f}$ mice expressed cell surface TCRα (Fig. 2C). Thus, deletion of Bim at the late DN to the early DP stage of development, confirmed by Bim-specific Ab staining (45) (Fig. 2D), results in increased levels of TCR$^+$DN thymocytes.

dLck promoter–driven late deletion of Bim does not enhance TCR$^+$DN thymocytes

To further narrow the time window in which the loss of Bim promotes TCR$^+$DN cells, we bred Bim$^{f/f}$ mice with dLckCre mice, in which Cre is expressed very late in the DP stage (46). Strikingly, the percentages and numbers of DN1–4, DP, CD4SP, and CD8SP cells were all normal in dLckCre$^+$Bim$^{f/f}$ mice, and there was no difference in cell surface TCRβ levels in DN thymocytes between WT and dLckCre$^+$Bim$^{f/f}$ mice (Fig. 3A). To confirm the efficiency of Bim deletion in dLckCre$^+$Bim$^{f/f}$ mice, Bim levels in thymocytes were assessed by flow cytometry. Most DP and DN thymocytes in dLckCre$^+$Bim$^{f/f}$ mice expressed normal levels of Bim, as did CD4$^+$CD8^{lo} intermediate stage thymocytes (Fig. 3B). A significant decrease in Bim was observed in a fraction of CD4SP and CD8SP thymocytes (Fig. 3B). However, the loss of Bim was nearly complete (~90% loss) in peripheral CD4$^+$, CD8$^+$ T cells in the spleen (Fig. 3B). Further division of the SP stage according to CCR7 and CD24 expression showed that Bim deletion starts at the SP1 (CCR7$^-$CD24^{hi}) stage and continues in later SP2 (CCR7$^+$CD24^{hi}) and SP3 (CCR7$^+$CD24^{lo}) stages (Fig. 3C), indicating that TCR$^+$DN thymocytes are derived from cortical DP cells, but not medullary SP cells. In addition to dLckCre$^+$Bim$^{f/f}$ mice, we also generated dLckCre$^+$Bax$^{f/f}$Bak$^{-/-}$ mice and found that these mice also did not have an accumulation of TCR$^+$DN cells (Supplemental Fig. 1B), unlike mice that have an earlier deletion of Bax (and Bak, LckCre$^+$Bax$^{f/f}$Bak$^{-/-}$) (Supplemental Fig. 1A). Together with the data in CD4Cre$^+$Bim$^{f/f}$ mice, these data are consistent with the concept that thymocytes avoiding Bim-driven apoptosis at the early DP stage downregulate CD4 and CD8 coreceptors and emerge as TCRαβ$^+$ DN cells, identifying a spatiotemporal role of Bim in the thymic selection of TCR$^+$DN cells.

In addition to TCR$^+$ DN thymocytes, other agonist-selected T cell populations may also be limited by Bim at a particular time during development. We observed that the CD4$^+$CD25$^-$Foxp3$^+$ thymocytes, which belong one of the precursor populations of Foxp3$^+$ Treg cells (47), were substantially increased in the Bim$^{-/-}$ or CD4Cre$^+$Bim$^{f/f}$ mice, but only subtly increased in dLckCre$^+$Bim$^{f/f}$ mice (Fig. 3D). Thus, the temporal expression of Bim contributes to multiple agonist-selected populations in the thymus.

TCR$^+$DN thymocytes express the postselection, immature phenotype and inefficiently develop into DP thymocytes

To further characterize the features of these TCR$^+$DN thymocytes, we first analyzed the expression of the postselection marker CD5 (48) on CD25$^-$CD44$^-$ DN4-like thymocytes from WT and Bim$^{-/-}$ mice. Compared to DN4 cells in WT mice, most of the DN4-like cells express CD5 in Bim$^{-/-}$ mice (Fig. 4A). Additionally, the DN thymocytes in Bim$^{-/-}$ mice express higher levels of S1pr1, Klf2, and CCR7 than DN thymocytes in WT mice (Supplemental Fig. 1C, 1D), suggesting their postselection state (49). Second, DN4-like cells from Bim$^{-/-}$ mice also expressed high levels of the immature marker CD24, suggesting that these accumulated TCR$\alpha\beta^+$ thymocytes are not mature recirculating peripheral T cells (Fig. 4B). Third, we determined whether Bim$^{-/-}$ DN4-like cells were capable of differentiating into DP cells by sorting CD4$^-$CD8$^-$CD25$^-$ CD44$^-$ DN thymocytes from WT or Bim$^{-/-}$ mice and culturing them with OP9-DL1 cells and IL-7. At 1 and 2 d after culture, the cells were harvested and assessed for expression of CD4 and CD8 by flow cytometry. Whereas DN4 cells from WT mice efficiently developed into DP cells, DN4-like cells from Bim$^{-/-}$ mice were largely unable to develop into DP cells (Fig. 4C). Importantly, this developmental blockade was specific to DN4-like cells in Bim$^{-/-}$ mice, as sorted DN1–3 cells from Bim$^{-/-}$ thymi progressed into DP cells when cultured with OP9-DL1 and IL-7 (Fig. 4D). Thus, TCR$^+$ DN thymocytes in Bim$^{-/-}$ mice displayed markers suggesting they were postselected, but still immature, thymocytes and that they were incapable of further developing into DP cells in OP9-DL1 culture.

Bim deletion results in agonist-selected T cell accumulation in the spleen with distinct TCR repertoire

After leaving thymi, the recent thymic emigrants populate the secondary lymphoid organs (13), so we examined the presence of TCR$^+$DN cells in the spleens of WT and Bim$^{-/-}$ mice. Strikingly, Bim$^{-/-}$ mice, or CD4Cre$^+$Bim$^{f/f}$ mice, had a 4- to 6-fold increase in TCR$^+$DN T cells compared with WT mice (Fig. 5A, Supplemental Fig. 2A). Interestingly, this increase in TCR$^+$DN T cells was not observed in dLckCre$^+$Bim$^{f/f}$ mice, in which the Bim deletion occurs at the late DP stage (Fig. 5B). One potential fate of thymic TCR$^+$DN cells is their further development into TCR$\alpha\beta^+$ CD8$\alpha\alpha$ iIELs (11). In the spleen, there was also a significant increase in TCR$\alpha\beta^+$ CD8$\alpha\alpha$ cells in Bim$^{-/-}$ mice, but not in dLckCre$^+$Bim$^{f/f}$ mice, although the cells are not as numerous as the DN T cells (Fig. 5A, 5B). Collectively, our data suggest that the accumulation of DN T and TCR$\alpha\beta^+$ CD8$\alpha\alpha$ cells is determined by Bim-mediated early thymic development.

Recent studies suggested that Bim is required for deleting TRA-reactive thymocytes in TCR-transgenic models (22–24). However, the effects of Bim in shaping the polyclonal TCR repertoire has not been fully studied. Therefore, we identified the polyclonal Ag-binding sequence (CDR3) of the TCRβ-chain by next-generation sequencing of purified DN T cells as well as CD4$^+$ and CD8$^+$ T cells (Supplemental Table I). Strikingly, PCA of V-J gene usage indicates that Bim controls TCRβ V-J chain usage in DN T cells, but not in conventional CD4 or CD8 T cells (Fig. 5C). These differences were not due to the effects of Bim on endogenous SAg-induced negative selection, because the TCRβ V-J chain usage in DN T cells remained different between C57BL/6 and Bim$^{-/-}$ mice after excluding all known

endogenous mouse mammary tumor virus SAg-reactive Vβ gene segments (for C56BL/6 mice: TRBV12, TRBV16, and TRBV24) (40, 50, 51) from PCA (Fig. 5D). Surprisingly, we observed that DN T cells, but not conventional T cells, have shorter CDR3 regions in $Bim^{-/-}$ mice (Fig. 5E, Supplemental Fig. 3A), which were results of fewer N-insertion nucleotides, instead of bias to shorter Vβ-chains (Supplemental Fig. 3B, 3C). The data showed that characteristic features of CDR3β sequences of DN T cells exist that are likely controlled by Bim. To determine whether distinct CDR3β sequences would accumulate in DN T cells from $Bim^{-/-}$ mice, we identified the number of CDR3β public sequences (i.e., those that are shared by different individuals). Interestingly, fewer CDR3β sequences of DN T cells are shared by different individual $Bim^{-/-}$ mice, as the number of private CDR3β sequences is significantly increased in individual $Bim^{-/-}$ mice (Fig. 5F). Notably, we did not find enrichment in private sequences in conventional T cells from $Bim^{-/-}$ mice (data not shown). In summary, these data show that Bim significantly limits the population size of DN T cells and restricts their private TCRβ repertoires.

Bim deletion rescues the splenic DN T cells, but not iIELs, in IL-15 knockout mice

We next examined whether the absence of Bim affected the accumulation of both DN T cells and CD8αα T cells in the intestinal epithelium. Similar to a previous report (13), mice deficient in Bim accumulated both DN T and CD8αα T cells in the iIEL compartment (Fig. 6A). Importantly, both DN and CD8αα iIELs were not increased in $dLckCre^{+}Bim^{f/f}$ mice (Fig. 6B). Thus, these data show that Bim expression in the thymus is an important limiting factor for both the splenic and intestinal accumulation of DN and CD8αα iIELs.

Previous studies suggested that Bim may also regulate the homeostasis of CD8αα T cells by antagonizing IL-15-induced Bcl-2 upregulation (27, 34, 35, 52). However, this antagonism is more evident in the periphery, as the loss of IL-15 does not substantially impair the development of TCR^{+}DN thymocytes (10, 27, 31). Consistent with these prior data, the frequencies of CD4SP, CD8SP, DP, or DN cells were not different between $IL\text{-}15^{-/-}$ and C57BL/6 mice (Supplemental Fig. 1E). Furthermore, the combined loss of IL-15 and Bim was not different compared with the loss of Bim alone in the accumulation of TCR^{+}DN thymocytes (Supplemental Fig. 1F).

Whereas IL-15 is not required for the thymic development of TCR^{+}DN thymocytes, it is critical for the postthymic homeostasis of CD8αα T cells, especially in the intestinal epithelium (29–31). Therefore, we further analyzed the DN and CD8αα T cells in the spleens and intestines of WT, $Bim^{-/-}$, $IL\text{-}15^{-/-}$, and $Bim^{-/-}IL\text{-}15^{-/-}$ mice. The $IL\text{-}15^{-/-}$ mice had a minor decrease in the frequency and number of splenic DN T cells but a significant loss of the CD8αα T cell population (Fig. 6C). Strikingly, the additional loss of Bim rescued both the splenic DN T and CD8αα T cell populations in $IL\text{-}15^{-/-}$ mice, and it failed to restore the intestinal intraepithelial DN or CD8αα T cells (Fig. 6C, 6D). Taken together, these data show that splenic DN T and CD8αα T cells are determined in the thymus and are limited by the presence of Bim, but that Bim is not the only IL-15 antagonist once the DN T and CD8αα cells reach the iIEL compartment.

Expression of CD8α, $\alpha_4\beta_7$, and CCR9 in splenic TCR$^+$DN cells are induced by anti-CD3/CD28 stimulation and/or IL-15

Previous studies have suggested that CD8αα iIELs are derived from thymic TCR$^+$DN cells (7, 11, 14, 25, 30), although how the cells migrate from the thymus to the gut is less well understood. In this study, we observed that TCR$^+$DN thymocytes in Bim$^{-/-}$ mice upregulated their S1pr1 expression, which facilitates their egress from the thymus (Supplemental Fig. 1C). One recent report showed that thymic emigrants, including DN T cells, populate the spleen before they populate the intestine (13). Given that IL-15 is critical for the survival and proliferation of CD8αα in the iIELs, and that the additional loss of Bim was able to restore CD8αα in the spleen but not the iIEL, we hypothesized that the splenic DN population is an intermediate stage between thymic TCR$^+$DN cells and intestinal CD8αα iIELs, and that IL-15 is critical for their transition from DN T to CD8αα cells.

To test these possibilities, splenic TCRβ$^+$CD4$^-$CD8$^-$ DN T cells from Bim$^{-/-}$ mice were isolated, cultured with IL-15, and analyzed by flow cytometry. IL-15 significantly induced the gut-homing chemokine receptor CCR9 and integrin $\alpha_4\beta_7$, in both expression level and frequency of expressing cells (Fig. 7A). We next reasoned that IL-15 may contribute to the expression of the CD8α. To test this, we sorted DN T cells from the spleen and stimulated them with anti-CD3/CD28 with and without IL-15. Either IL-15 or anti-CD3/28 stimulation promoted the expression of CD8α. Together, they synergistically enhanced CD8α expression by DN T cells (Fig. 7B). To further support this concept, we took advantage of Nur77^{GFP} mice, in which the magnitude of GFP expression can reflect the intensity of TCR stimulation (53). Ex vivo splenic CD8αα T cells isolated from Nur77^{GFP} mice expressed high levels of GFP, indicating that they receive strong TCR stimulation, which drives their transition from DN T to CD8αα T cells (Supplemental Fig. 2B). To determine whether Stat5, a critical IL-15 signal transducer, was important for CD8α induction, we took advantage of dLckCre$^+$Stat5$^{f/f}$ mice (32). To enhance the survival of Stat5^{low} cells, we additionally crossed dLckCre$^+$Stat5$^{f/f}$ mice to Bim$^{f/f}$ mice. Purified splenic DN T cells from WT, dLckCre$^+$Bim$^{f/f}$, or dLckCre$^+$Stat5$^{f/f}$Bim$^{f/f}$ mice were stimulated with anti-CD3/CD28 and/or IL-15. The deletion of Stat5 significantly reduced the emergence of CD8α-expressing cells in response to either anti-CD3/28 or IL-15 alone or in combination (Fig. 7B), whereas the DN T cells from dLckCre$^+$ Bim$^{f/f}$ mice had the same potential to develop into CD8αα T cells as WT cells (data not shown). As we previously observed that the deletion of Stat5 in dLckCre$^+$Stat5$^{f/f}$ mice was not complete (32), we again found that >30% of the DN T cells from dLckCre$^+$ Stat5$^{f/f}$ Bim$^{f/f}$ mice were Stat5^{low}, and that culture with IL-15 led to a selection for Stat5-expressing cells that also expressed CD8α (Supplemental Fig. 2C).

To definitively test whether DN T cells from the spleen could give rise to CD8αα T cells in vivo, we took advantage of Bim$^{-/-}$ mice as donors because of their abundant DN T cell population and transferred purified DN T cells (Fig. 7C) into congenically marked CD45.1$^+$BoyJ recipients and tracked the transferred cells 1 wk later. In the spleen, mesenteric lymph node, and intestinal epithelium, most donor cells maintained a low expression of CD8α (Fig. 7D). However, in all mice analyzed, we saw the emergence of a small proportion of donor cells in the spleen and mesenteric lymph node, as well as a large population of donor cells in the iIELs, that expressed CD8α (Fig. 7D). Collectively, these

data show that splenic DN T cells are the precursors of intestinal CD8αα iIELs, whose transition is promoted by IL-15/STAT5 signaling.

Discussion

Our data show that timed deletion of Bim promotes the development of TCRaβ$^+$ DN thymocytes. Although it is possible that these TCR$^+$DN thymocytes could be misdirected SP thymocytes or recirculating T cells from the periphery, our data suggest that neither of these mechanisms contributes in a substantial way to the accumulation of TCR$^+$DN thymocytes. Indeed, these TCR$^+$DN cells 1) express the immature marker CD24; 2) are increased when Bim is deleted early, but not late, in the DP stage; and 3) have a balanced expression of Th-Pok and Runx3 (Supplemental Fig. 1G), whereas the CD4SP and CD8SP cells have high levels of Th-Pok and Runx3 expression, respectively. Instead, our data suggest that the TCR$^+$DN thymocytes in Bim $^/$ mice are derived from DP cells that escaped negative selection. Several pieces of data support this conjecture. First, the sorted DN1-DN3 thymocytes from Bim$^{-/-}$ mice progressed through the DP stage in OP9-DL1 culture. Second, TCR$^+$DN cells accumulated in CD4Cre$^+$ Bim$^{f/f}$ mice, but not in dLckCre$^+$Bim$^{f/f}$ mice, demonstrating that expression of CD4 is a prerequisite for the accrual of TCR$^+$DN cells. Third, the TCR$^+$DN cells expressed a postselection marker, consistent with data from other studies showing that the TCR$^+$DN thymocytes express postselection or activated markers (13, 14, 25). Finally, strong TCR stimulation from self-peptide/MHC can lead to loss of CD4 and CD8 expression, which can be difficult to observe unless apoptosis is prevented (17, 48, 54, 55). Collectively, these data support the idea that the DN4-like thymocytes with surface TCRαβ expression, which are limited by Bim, once expressed coreceptors and had progressed to at least the DP stage.

A few non-mutually exclusive explanations may help clarify the controversy surrounding the role of Bim in thymocyte negative selection. First, one study showed that Bim and Puma function cooperatively to control thymocyte apoptosis to self-antigen (22). However, we failed to observe a substantial difference in endogenous SAg-reactive TCR$^+$DN thymocytes or in T cells (data not shown) between Bim$^{-/-}$ or LckCre$^+$Bax$^{f/f}$Bak$^{-/-}$ mice and WT mice. Another possibility is that Nur77 and/or other proapoptotic factors mediated cell death may also compensate for the loss of Bim and eliminate UbA- or SAg-reactive cells before they enter the thymic medulla (24, 56, 57). These hypotheses require further experimentation. Nonetheless, our data from the CD4-Cre- or dLck-Cre-driven conditional knockout models suggest a unique role for Bim in limiting the development of TCR$^+$DN thymocytes at the DP stage. Additionally, LckCre$^+$Bax$^{f/f}$Bak$^{-/-}$ mice have the same thymic phenotype with Bim$^{-/-}$ mice, showing that Bim has a dominant role among BH3-only proapoptotic factors in limiting TCR$^+$DN thymocytes. These accumulated cells likely bear TCRs that are of very high avidity to self-peptide/MHC agonistic Ags and drive coreceptor downregulation, which make them acquire a TCRα$^+$β$^+$CD5$^+$ DN phenotype, with high levels of Klf2, S1pr1, and CCR7. This TCR stimulation–induced DN phenotype is similarly observed in several in vitro thymocyte differentiation models (11, 44, 57) and in vivo mouse models (13, 14, 24, 57) that employ strong TCR stimulation. A potential physiologic reason for the downregulation of CD4 and CD8 during strong TCR interactions would be to reduce the overall avidity of thymocytes that may have significant self-reactivity.

The self-reactive TCR$^+$DN thymocytes can also be observed in WT mice, although they are lower in frequency and cell number. These cells have been previously considered to be the products of agonist selection, in which the interaction with strong agonistic self-antigen in the thymus promotes their development with minimal negative selection (7, 11, 13, 14). CD4$^+$Foxp3$^+$ Tregs, iNKT cells, and TCRαβ CD8αα iIELs have been reported to develop via this pathway (reviewed in Ref. 12). It remains unclear at which stage the agonist selection of TCR$^+$DN thymocytes occurs and why some self-reactive thymocytes undergo agonist selection rather than negative selection. A previous study suggested the TCR$^+$DN thymocytes are derived from CD4^{hi}CD8^{1o} Int thymocytes, the Ag-experienced DP cells that are making CD4/CD8 lineage choice, based on their endogenous SAg-reactive TCRβ repertoire (25). In this study, our temporal- and cell-specific conditional knockout models provide direct evidence that Bim plays a critical role in the decision of agonist versus negative selection during the DP stage, which would encompass the CD4^{hi} CD8^{1o} stage. Thus, the cell-intrinsic function of Bim particularly at the early DP, but not late DP or SP stage, critically limits the development of TCR$^+$DN thymocytes, the precursors of CD8αα iIELs.

The Ags inducing agonist selection of TCR$^+$DN thymocytes have not been well characterized. One possibility is that Aire-dependent TRA expression promotes agonist selection of TCR$^+$ DN thymocytes. However, in the absence of Aire, there was no accumulation of DN thymocytes (58, 59). Furthermore, prior work in TCR-transgenic models showed that the loss of Bim did not enlarge the TRA-specific DN thymocyte population (22–24). Indeed, we found significant Bim deletion as early as the SP1 (CCR7$^-$) cortical stage and even more striking in the SP2–3 (CCR7$^+$) medullary stage in dLckCre$^+$Bim$^{f/f}$ mice. Despite this substantial reduction in Bim in SP2–3 medullary thymocytes, we failed to observe an accumulation of TCR$^+$DN thymocytes, peripheral DN T, or CD8αα T cells, suggesting a minor role for medullary TRA in Bim-limited agonist selection. Together with the data from CD4Cre$^+$Bim$^{f/f}$ mice, our polyclonal TCR study provides strong evidence supporting the concept that UbA or SAg expressed in the cortex or cortical-medullary junction plays a critical role in Bim-limited agonist selection of TCR$^+$DN thymocytes.

It remains possible that TRA can induce agonist selection in the thymic medulla that may contribute to the development of Tregs or iNKT cells. One of the precursor populations of Foxp3$^+$ Treg cells, CD25$^-$Foxp3$^+$ CD4SP thymocytes, is limited by Bim (47). In this study, we further used CD4Cre- and dLckCre-driven Bim deletion to show that cortical expression of Bim may substantially limit CD25$^-$Foxp3$^+$ Treg precursors. Also, CD25$^-$Foxp3$^+$ Treg precursor accumulation in dLckCre$^+$Bim$^{f/f}$ mice may reflect the role of Bim in limiting medullary Aire-driven selection of Tregs (60), which differs from the development of TCR$^+$DN thymocytes that is limited by cortical Bim expression. This enhancement of CD25$^-$Foxp3$^+$ Treg precursors in the absence of Bim may explain the relative resistance of Bim-deficient mice to the development of spontaneous autoimmunity. Indeed, in our previous study we found that Bim limits the peripheral effector Treg-expressing CD25^{10}Foxp3$^+$ phenotype (61), even though its thymic precursors have not been carefully identified. The peripheral distribution and function of these CD25$^-$Foxp3$^+$ thymocyte-derived Treg cells require further investigation.

In the present study, we also found that Bim not only limits the population size of agonist-selected DN T cells but also shapes their TCR repertoire. In this study, we analyzed the TCR repertoire by high-throughput sequencing and bioinformatics analysis. The results show that the accumulation of TCR^+DN thymocytes and DN T cells in $Bim^{-/-}$ mice is not a random process, which affects all cells similarly. Instead, our data show that Bim-deficient DN T cells have 1) distinct TCRβ V-J chain usage, 2) shorter CDR3 lengths, and 3) increased numbers of private CDR3 sequences. In contrast to prior studies using monoclonal TCR-transgenic mice (20, 22–24), in the present study we found little evidence that Bim constricts the TCRβ repertoire of conventional $CD4^+$ or $CD8^+$ T cells. However, it remains possible that Bim affects the TCRα repertoire.

Consistent with a previous study that reported that CDR3 lengths are not altered by thymic selection (62), we observed that CDR3 lengths of $CD4^+$ or $CD8^+$ T cells remain the same in $Bim^{-/-}$ mice. Surprisingly, we found that the CDR3 lengths in Bim-deficient DN T cells were shorter than those from C57BL/6 mice. One possible explanation for this observation might be that shorter CDR3 lengths have less discriminatory power in peptide recognition. These TCRs with short CDR3 may interact more broadly with peptides presented by MHC, increasing their cross-reactivity. In line with this, previous studies showed that negative selection limits TCR cross-reactivity and hones the repertoire toward the peptides (15, 63, 64). This makes some teleological sense in that highly promiscuous TCRs should be eliminated prior to their export into the periphery where they might be triggered by multiple ligands. With regard to the biological meaning of these shorter CDR3s, prior studies showed that TCRs bearing shorter CDR3 lengths tend to dominate the activated T cell population in experimentally induced allergic encephalomyelitis models (65, 66), suggesting that CDR3 length may determine the TCR reactivity to self-antigens. Alternatively, it is possible that the accumulation of DN T cells in $Bim^{-/-}$ mice starts at the neonatal period when the TdT was not activated. Without TdT, the CDR3 regions of neonatal T cells are shorter than those of adult T cells (67, 68). It is possible that the early generated T cells with shorter CDR3 lengths survive better and accumulate in the absence of Bim, and their enrichment contributes to the shorter CDR3 lengths in the population.

Although our data show that Bim expression at the DP stage limits the production of DN cells, how these cells acquire CD8αα expression and migrate to the gut has not been clearly defined. Several studies showed that TCR^+DN thymocytes in vitro cultured with IL-15 can acquire a CD8αα iIEL-like phenotype (11, 25, 27). However, the absence of IL-15 does not lead to the loss of DN T cells in the thymus; thus, the effects of IL-15 on thymocytes in vitro may not recapitulate the effects of IL-15 in vivo. Instead, other work shows that IL-15 is critical for maintenance of CD8αα iIELs in the periphery (10, 27, 28, 30, 31), either by promoting their peripheral development, migration, and/or survival. Previous studies provided strong evidence that TCR^+DN thymocytes when adoptively transferred could develop into CD8αα iIELs in vivo (11, 25, 30), whereas the intestinal epithelial cells can functionally transpresent IL-15 (30). In the present study, we found that TCR^+ DN thymocytes expressed S1pr1, which facilitates thymic egress. Additionally, a recent in vivo labeling experiment showed that the CD8αα iIEL precursors migrate to secondary lymphoid organs (SLOs) in the first 24 h after leaving thymus and are present there as TCR^+DN T cells. Importantly, these cells were not observed in the intestinal epithelium at this time (13).

Taken together, these data suggest that DN T cells in secondary lymphoid organs must undergo additional maturation into CD8αα T cells either in the SLOs or when they arrive in the intestine. Indeed, our data show that splenic DN T cells can undergo significant transition into CD8αα T cells both in vitro and in vivo. However, the expression of CD5, CD25, and CD44 on splenic DN T cells is not identical between WT and $Bim^{-/-}$ mice (Supplemental Fig. 2D). It is likely that the cells with dysregulated expression of these molecules represent cells that are eliminated by Bim during the process of agonist selection. Additionally, accumulated DN T cells may not receive enough environmental stimulation for maturation because the DN T niche may be limited. In support of this scenario, both CD25 and CD44 are significantly lower in $Bim^{-/-}$ peripheral DN T cells. Additionally, CD5 has not been repressed in $Bim^{-/-}$ DN T cells, suggesting that these cells have not yet fully matured as WT DN T cells but still have emigrated to the spleen. Furthermore, we identified another role for IL-15, which is to synergistically enhance the TCR-driven CD8αα expression on DN T cells in a Stat5-dependent manner, suggesting that splenic DN T cells are in an intermediate stage between TCR^{+}DN thymocytes and CD8αα iIELs. Our data are consistent with prior work showing that $CD4^{-}CD8\beta^{-}$ splenic T cells expressing a transgenic TCR cloned from iIELs can develop into iIELs in a lymphopenic environment (14). Importantly, our experiments were done using $CD4^{-}CD8\alpha^{-}$ DN splenic T cells with a natural TCR repertoire and were performed in immune-intact mice. Thus, these data provide strong evidence in support of a model in which DN T cells are precursors of CD8αα iIELs that can undergo additional maturation in the SLOs and/or intestine.

Previous studies suggested that Bim is involved in regulating apoptosis of CD8αα iIELs via antagonizing IL-15–induced prosurvival effects (27, 34, 35). Indeed, anti-apoptotic Bcl-2 upregulation heavily depends on IL-15 transpresentation in the intestinal epithelium (30). However, we observed that the additional deletion of Bim did not restore CD8αα iIELs in IL-15–deficient mice. These data suggest that IL-15 combats Bim and perhaps other proapoptotic molecules, such as Puma and Noxa (36). Indeed, a previous in vitro study showed that the absence of Bim can only partially protect CD8αα iIELs from IL-15 starvation-induced apoptosis (34). IL-15 also promotes CD8αα iIEL proliferation, which expands its population (52). Furthermore, IL-15 promotes the expression of E-cadherin on epithelial cells (69), which is important for iIEL retention after they migrate into the gut (70). IL-15 also contributes to the intestinal niche for iIEL by promoting intestinal epithelial cell proliferation and survival (71, 72). Thus, although Bim controls the thymic selection of CD8αα iIEL precursors, it cannot compensate for the loss of IL-15 on the intestinal maintenance of these cells.

This study further illustrates the role of Bim during thymic development. Bim critically and stage specifically controls the agonist selection of an unconventional T cell population and shapes its TCR repertoire. This study has implications for our understanding of the development and homeostasis of DN T and CD8αα T cells. Furthermore, the $CD4Cre^{+}Bim^{f/f}$ versus $dLckCre^{+}Bim^{f/f}$ mouse models may provide unique tools to investigate the role of CD8αα iIELs and other agonist-selected populations in gut infectious or autoimmune diseases.

Supplementary Material

Refer to Web version on PubMed Central for supplementary material.

Acknowledgments

We thank Dr. Andrew Herr and members of the Hildeman laboratory for helpful discussions and apologize to those whose work was not cited due to reference limits.

This work was supported by Public Health Service Grant R01AI057753 (to D.A.H.), as well as by International Research Training Group 1911, Sonderforschungsbereich 654, and Excellence Cluster Inflammation at Interfaces EXC306 from the German Research Foundation.

Abbreviations used

BoyJ	B6.SJL-*Ptprc*^{a}*Pepc*^{b}/BoyCrCrl
DN	double-negative
DP	double-positive
IEL	intraepithelial lymphocyte
iIEL	intestinal intraepithelial lymphocyte
MHC II	MHC class II
PCA	principal component analysis
SAg	superantigen
SLO	secondary lymphoid organ
SP	single-positive
TRA	tissue-restricted self-antigen
Treg	regulatory T cell
UbA	ubiquitous self-antigen
WT	wild-type

References

1. Juvet SC, Zhang L. Double negative regulatory T cells in transplantation and autoimmunity: recent progress and future directions. J Mol Cell Biol. 2012; 4:48–58. [PubMed: 22294241]
2. Poussier P, Ning T, Banerjee D, Julius M. A unique subset of self-specific intraintestinal T cells maintains gut integrity. J Exp Med. 2002; 195:1491–1497. [PubMed: 12045247]
3. Wei B, Velazquez P, Turovskaya O, Spricher K, Aranda R, Kronenberg M, Birnbaumer L, Braun J. Mesenteric B cells centrally inhibit CD4^{+} T cell colitis through interaction with regulatory T cell subsets. Proc Natl Acad Sci USA. 2005; 102:2010–2015. [PubMed: 15684084]
4. Cheroutre H, Lambolez F, Mucida D. The light and dark sides of intestinal intraepithelial lymphocytes. Nat Rev Immunol. 2011; 11:445–456. [PubMed: 21681197]

5. Rocha B, Vassalli P, Guy-Grand D. The V beta repertoire of mouse gut homodimeric alpha CD8$^+$ intraepithelial T cell receptor alpha/beta$^+$ lymphocytes reveals a major extrathymic pathway of T cell differentiation. J Exp Med. 1991; 173:483–486. [PubMed: 1824858]
6. Rocha B. The extrathymic T-cell differentiation in the murine gut. Immunol Rev. 2007; 215:166–177. [PubMed: 17291287]
7. Leishman AJ, Gapin L, Capone M, Palmer E, MacDonald HR, Kronenberg M, Cheroutre H. Precursors of functional MHC class I- or class II-restricted CD8αα$^+$ T cells are positively selected in the thymus by agonist self-peptides. Immunity. 2002; 16:355–364. [PubMed: 11911821]
8. Guy-Grand D, Azogui O, Celli S, Darche S, Nussenzweig MC, Kourilsky P, Vassalli P. Extrathymic T cell lymphopoiesis: ontogeny and contribution to gut intraepithelial lymphocytes in athymic and euthymic mice. J Exp Med. 2003; 197:333–341. [PubMed: 12566417]
9. Lambolez F, Kronenberg M, Cheroutre H. Thymic differentiation of TCRαβ$^+$ CD8αα$^+$ IELs. Immunol Rev. 2007; 215:178–188. [PubMed: 17291288]
10. Klose CSN, Blatz K, d'Hargues Y, Hernandez PP, Kofoed-Nielsen M, Ripka JF, Ebert K, Arnold SJ, Diefenbach A, Palmer E, Tanriver Y. The transcription factor T-bet is induced by IL-15 and thymic agonist selection and controls CD8αα$^+$ intraepithelial lymphocyte development. Immunity. 2014; 41:230–243. [PubMed: 25148024]
11. Gangadharan D, Lambolez F, Attinger A, Wang-Zhu Y, Sullivan BA, Cheroutre H. Identification of pre- and postselection TCRαβ$^+$ intraepithelial lymphocyte precursors in the thymus. Immunity. 2006; 25:631–641. [PubMed: 17045820]
12. Stritesky GL, Jameson SC, Hogquist KA. Selection of self-reactive T cells in the thymus. Annu Rev Immunol. 2012; 30:95–114. [PubMed: 22149933]
13. McDonald BD, Bunker JJ, Ishizuka IE, Jabri B, Bendelac A. Elevated T cell receptor signaling identifies a thymic precursor to the TCRαβ$^+$ CD4 CD8β intraepithelial lymphocyte lineage. Immunity. 2014; 41:219–229. [PubMed: 25131532]
14. Mayans S, Stepniak D, Palida SF, Larange A, Dreux J, Arlian BM, Shinnakasu R, Kronenberg M, Cheroutre H, Lambolez F. αβT cell receptors expressed by CD4$^-$CD8αβ$^-$ intraepithelial T cells drive their fate into a unique lineage with unusual MHC reactivities. Immunity. 2014; 41:207–218. [PubMed: 25131531]
15. McDonald BD, Bunker JJ, Erickson SA, Oh-Hora M, Bendelac A. Crossreactive αβ T cell receptors are the predominant targets of thymocyte negative selection. Immunity. 2015; 43:859–869. [PubMed: 26522985]
16. Klein L, Kyewski B, Allen PM, Hogquist KA. Positive and negative selection of the T cell repertoire: what thymocytes see (and don't see). Nat Rev Immunol. 2014; 14:377–391. [PubMed: 24830344]
17. Starr TK, Jameson SC, Hogquist KA. Positive and negative selection of T cells. Annu Rev Immunol. 2003; 21:139–176. [PubMed: 12414722]
18. Bouillet P, Purton JF, Godfrey DI, Zhang LC, Coultas L, Puthalakath H, Pellegrini M, Cory S, Adams JM, Strasser A. BH3-only Bcl-2 family member Bim is required for apoptosis of autoreactive thymocytes. Nature. 2002; 415:922–926. [PubMed: 11859372]
19. Hutcheson J, Scatizzi JC, Bickel E, Brown NJ, Bouillet P, Strasser A, Perlman H. Combined loss of proapoptotic genes Bak or Bax with Bim synergizes to cause defects in hematopoiesis and in thymocyte apoptosis. J Exp Med. 2005; 201:1949–1960. [PubMed: 15967824]
20. Hu Q, Sader A, Parkman JC, Baldwin TA. Bim-mediated apoptosis is not necessary for thymic negative selection to ubiquitous self-antigens. J Immunol. 2009; 183:7761–7767. [PubMed: 19933852]
21. Jorgensen TN, McKee A, Wang M, Kushnir E, White J, Refaeli Y, Kappler JW, Marrack P. Bim and Bcl-2 mutually affect the expression of the other in T cells. J Immunol. 2007; 179:3417–3424. [PubMed: 17785775]
22. Gray DHD, Kupresanin F, Berzins SP, Herold MJ, O'Reilly LA, Bouillet P, Strasser A. The BH3-only proteins Bim and Puma cooperate to impose deletional tolerance of organ-specific antigens. Immunity. 2012; 37:451–462. [PubMed: 22960223]

23. Suen AYW, Baldwin TA. Proapoptotic protein Bim is differentially required during thymic clonal deletion to ubiquitous versus tissue-restricted antigens. Proc Natl Acad Sci USA. 2012; 109:893–898. [PubMed: 22215602]
24. Daley SR, Hu DY, Goodnow CC. Helios marks strongly autoreactive $CD4^+$ T cells in two major waves of thymic deletion distinguished by induction of PD-1 or NF-κB. J Exp Med. 2013; 210:269–285. [PubMed: 23337809]
25. Pobezinsky LA, Angelov GS, Tai X, Jeurling S, Van Laethem F, Feigenbaum L, Park JH, Singer A. Clonal deletion and the fate of autoreactive thymocytes that survive negative selection. Nat Immunol. 2012; 13:569–578. [PubMed: 22544394]
26. Hutcheson J, Perlman H. Loss of Bim results in abnormal accumulation of mature CD4 CD8 CD44 CD25 thymocytes. Immunobiology. 2007; 212:629–636. [PubMed: 17869640]
27. Jiang W, Ferrero I, Laurenti E, Trumpp A, MacDonald HR. c-Myc controls the development of CD8αα TCRαβ intestinal intraepithelial lymphocytes from thymic precursors by regulating IL-15-dependent survival. Blood. 2010; 115:4431–4438. [PubMed: 20308599]
28. Kennedy MK, Glaccum M, Brown SN, Butz EA, Viney JL, Embers M, Matsuki N, Charrier K, Sedger L, Willis CR, et al. Reversible defects in natural killer and memory CD8 T cell lineages in interleukin 15-deficient mice. J Exp Med. 2000; 191:771–780. [PubMed: 10704459]
29. Schluns KS, Nowak EC, Cabrera-Hernandez A, Puddington L, Lefrancois L, Aguila HL. Distinct cell types control lymphoid subset development by means of IL-15 and IL-15 receptor α expression. Proc Natl Acad Sci USA. 2004; 101:5616–5621. [PubMed: 15060278]
30. Ma LJ, Acero LF, Zal T, Schluns KS. Trans-presentation of IL-15 by intestinal epithelial cells drives development of CD8αα IELs. J Immunol. 2009; 183:1044–1054. [PubMed: 19553528]
31. Lai YG, Hou MS, Hsu YW, Chang CL, Liou YH, Tsai MH, Lee F, Liao NS. IL-15 does not affect IEL development in the thymus but regulates homeostasis of putative precursors and mature $CD8αα^+$ IELs in the intestine. J Immunol. 2008; 180:3757–3765. [PubMed: 18322181]
32. Tripathi P, Kurtulus S, Wojciechowski S, Sholl A, Hoebe K, Morris SC, Finkelman FD, Grimes HL, Hildeman DA. STAT5 is critical to maintain effector CD8+ T cell responses. J Immunol. 2010; 185:2116–2124. [PubMed: 20644163]
33. Kurtulus S, Tripathi P, Moreno-Fernandez ME, Sholl A, Katz JD, Grimes HL, Hildeman DA. Bcl-2 allows effector and memory $CD8^+$T cells to tolerate higher expression of Bim. J Immunol. 2011; 186:5729–5737. [PubMed: 21451108]
34. Lai YG, Hou MS, Lo A, Huang ST, Huang YW, Yang-Yen HF, Liao NS. IL-15 modulates the balance between Bcl-2 and Bim via a Jak3/1-PI3K-Akt-ERK pathway to promote $CD8αα^+$ intestinal intraepithelial lymphocyte survival. Eur J Immunol. 2013; 43:2305–2316. [PubMed: 23754237]
35. Malamut G, El Machhour R, Montcuquet N, Martin-Lanneree S, Dusanter-Fourt I, Verkarre V, Mention J-J, Rahmi G, Kiyono H, Butz EA, et al. IL-15 triggers an antiapoptotic pathway in human intraepithelial lymphocytes that is a potential new target in celiac disease-associated inflammation and lymphomagenesis. J Clin Invest. 2010; 120:2131–2143. [PubMed: 20440074]
36. Kurtulus S, Sholl A, Toe J, Tripathi P, Raynor J, Li KP, Pellegrini M, Hildeman DA. Bim controls IL-15 availability and limits engagement of multiple BH3-only proteins. Cell Death Differ. 2015; 22:174–184. [PubMed: 25124553]
37. Lefrancois L, Lycke N. Isolation of mouse small intestinal intraepithelial lymphocytes, Peyer's patch, and lamina propria cells. Curr Protoc Immunol. 2001 Chapter 3: Unit 3.19.
38. Phelan JD, Saba I, Zeng H, Kosan C, Messer MS, Olsson HA, Fraszczak J, Hildeman DA, Aronow BJ, Moroy T, Grimes HL. Growth factor independent-1 maintains Notch1-dependent transcriptional programming of lymphoid precursors. PLoS Genet. 2013; 9:e1003713. [PubMed: 24068942]
39. Bolotin DA, Shugay M, Mamedov IZ, Putintseva EV, Turchaninova MA, Zvyagin IV, Britanova OV, Chudakov DM. MiTCR: software for T-cell receptor sequencing data analysis. Nat Methods. 2013; 10:813–814. [PubMed: 23892897]
40. Lefranc M-P, Giudicelli V, Busin C, Malik A, Mougenot I, Dehais P, Chaume D. LIGM-DB/IMGT: an integrated database of Ig and TcR, part of the immunogenetics database. Ann N Y Acad Sci. 1995; 764:47–49. [PubMed: 7486568]

41. Warren RL, Freeman JD, Zeng T, Choe G, Munro S, Moore R, Webb JR, Holt RA. Exhaustive T-cell repertoire sequencing of human peripheral blood samples reveals signatures of antigen selection and a directly measured repertoire size of at least 1 million clonotypes. Genome Res. 2011; 21:790–797. [PubMed: 21349924]
42. Nazarov VI, Pogorelyy MV, Komech EA, Zvyagin IV, Bolotin DA, Shugay M, Chudakov DM, Lebedev YB, Mamedov IZ. tcR: an R package for T cell receptor repertoire advanced data analysis. BMC Bioinformatics. 2015; 16:175. [PubMed: 26017500]
43. Shimizu C, Kawamoto H, Yamashita M, Kimura M, Kondou E, Kaneko Y, Okada S, Tokuhisa T, Yokoyama M, Taniguchi M, et al. Progression of T cell lineage restriction in the earliest subpopulation of murine adult thymus visualized by the expression of lck proximal promoter activity. Int Immunol. 2001; 13:105–117. [PubMed: 11133839]
44. Wang R, Wang-Zhu Y, Grey H. Interactions between double positive thymocytes and high affinity ligands presented by cortical epithelial cells generate double negative thymocytes with T cell regulatory activity. Proc Natl Acad Sci USA. 2002; 99:2181–2186. [PubMed: 11842216]
45. Chougnet CA, Tripathi P, Lages CS, Raynor J, Sholl A, Fink P, Plas DR, Hildeman DA. A major role for Bim in regulatory T cell homeostasis. J Immunol. 2011; 186:156–163. [PubMed: 21098226]
46. Zhang DJ, Wang Q, Wei J, Baimukanova G, Buchholz F, Stewart AF, Mao X, Killeen N. Selective expression of the Cre recombinase in late-stage thymocytes using the distal promoter of the *Lck* gene. J Immunol. 2005; 174:6725–6731. [PubMed: 15905512]
47. Tai X, Erman B, Alag A, Mu J, Kimura M, Katz G, Guinter T, McCaughtry T, Etzensperger R, Feigenbaum L, et al. Foxp3 transcription factor is proapoptotic and lethal to developing regulatory T cells unless counterbalanced by cytokine survival signals. Immunity. 2013; 38:1116–1128. [PubMed: 23746651]
48. Groves T, Katis P, Madden Z, Manickam K, Ramsden D, Wu G, Guidos CJ. In vitro maturation of clonal $CD4^+CD8^+$ cell lines in response to TCR engagement. J Immunol. 1995; 154:5011–5022. [PubMed: 7730608]
49. Rivera J, Proia RL, Olivera A. The alliance of sphingosine-1-phosphate and its receptors in immunity. Nat Rev Immunol. 2008; 8:753–763. [PubMed: 18787560]
50. Scherer MT, Ignatowicz L, Winslow GM, Kappler JW, Marrack P. Superantigens: bacterial and viral proteins that manipulate the immune system. Annu Rev Cell Biol. 1993; 9:101–128. [PubMed: 7506550]
51. Lefranc MP, Giudicelli V, Busin C, Bodmer J, Muller W, Bontrop R, Lemaitre M, Malik A, Chaume D. IMGT, the International Im-MunoGeneTics database. Nucleic Acids Res. 1998; 26:297–303. [PubMed: 9399859]
52. Lai YG, Gelfanov V, Gelfanova V, Kulik L, Chu CL, Jeng SW, Liao NS. IL-15 promotes survival but not effector function differentiation of $CD8^+$ $TCR\alpha\beta^+$ intestinal intraepithelial lymphocytes. J Immunol. 1999; 163:5843–5850. [PubMed: 10570268]
53. Moran AE, Holzapfel KL, Xing Y, Cunningham NR, Maltzman JS, Punt J, Hogquist KA. T cell receptor signal strength in Treg and iNKT cell development demonstrated by a novel fluorescent reporter mouse. J Exp Med. 2011; 208:1279–1289. [PubMed: 21606508]
54. McGargill MA, Hogquist KA. Antigen-induced coreceptor down-regulation on thymocytes is not a result of apoptosis. J Immunol. 1999; 162:1237–1245. [PubMed: 9973375]
55. McCaughtry TM, Baldwin TA, Wilken MS, Hogquist KA. Clonal deletion of thymocytes can occur in the cortex with no involvement of the medulla. J Exp Med. 2008; 205:2575–2584. [PubMed: 18936237]
56. Hu QN, Baldwin TA. Differential roles for Bim and Nur77 in thymocyte clonal deletion induced by ubiquitous self-antigen. J Immunol. 2015; 194:2643–2653. [PubMed: 25687757]
57. Kovalovsky D, Pezzano M, Ortiz BD, Sant'Angelo DB. A novel TCR transgenic model reveals that negative selection involves an immediate, Bim-dependent pathway and a delayed, Bim-independent pathway. PLoS One. 2010; 5:e8675. [PubMed: 20072628]
58. Anderson MS, Venanzi ES, Klein L, Chen Z, Berzins SP, Turley SJ, von Boehmer H, Bronson R, Dierich A, Benoist C, Mathis D. Projection of an immunological self shadow within the thymus by the aire protein. Science. 2002; 298:1395–1401. [PubMed: 12376594]

59. Hubert F-X, Kinkel SA, Crewther PE, Cannon PZF, Webster KE, Link M, Uibo R, O'Bryan MK, Meager A, Forehan SP, et al. Aire-deficient C57BL/6 mice mimicking the common human 13-base pair deletion mutation present with only a mild autoimmune phenotype. J Immunol. 2009; 182:3902–3918. [PubMed: 19265170]
60. Malchow S, Leventhal DS, Nishi S, Fischer BI, Shen L, Paner GP, Amit AS, Kang C, Geddes JE, Allison JP, et al. Aire-dependent thymic development of tumor-associated regulatory T cells. Science. 2013; 339:1219–1224. [PubMed: 23471412]
61. Raynor J, Karns R, Almanan M, Li KP, Divanovic S, Chougnet CA, Hildeman DA. IL-6 and ICOS antagonize Bim and promote regulatory T cell accrual with age. J Immunol. 2015; 195:944–952. [PubMed: 26109645]
62. Rock EP, Sibbald PR, Davis MM, Chien YH. CDR3 length in antigen-specific immune receptors. J Exp Med. 1994; 179:323–328. [PubMed: 8270877]
63. Huseby ES, White J, Crawford F, Vass T, Becker D, Pinilla C, Marrack P, Kappler JW. How the T cell repertoire becomes peptide and MHC specific. Cell. 2005; 122:247–260. [PubMed: 16051149]
64. Huseby ES, Crawford F, White J, Kappler J, Marrack P. Negative selection imparts peptide specificity to the mature T cell repertoire. Proc Natl Acad Sci USA. 2003; 100:11565–11570. [PubMed: 14504410]
65. Gold DP, Offner H, Sun D, Wiley S, Vandenbark AA, Wilson DB. Analysis of T cell receptor beta chains in Lewis rats with experimental allergic encephalomyelitis: conserved complementarity determining region 3. J Exp Med. 1991; 174:1467–1476. [PubMed: 1836012]
66. Zhang XM, Heber-Katz E. T cell receptor sequences from en-cephalitogenic T cells in adult Lewis rats suggest an early ontogenic origin. J Immunol. 1992; 148:746–752. [PubMed: 1370515]
67. Gavin MA, Bevan MJ. Increased peptide promiscuity provides a rationale for the lack of N regions in the neonatal T cell repertoire. Immunity. 1995; 3:793–800. [PubMed: 8777724]
68. Gilfillan S, Benoist C, Mathis D. Mice lacking terminal deoxy-nucleotidyl transferase: adult mice with a fetal antigen receptor repertoire. Immunol Rev. 1995; 148:201–219. [PubMed: 8825288]
69. Giron-Michel J, Azzi S, Khawam K, Mortier E, Caignard A, Devocelle A, Ferrini S, Croce M, Francois H, Lecru L, et al. Interleukin-15 plays a central role in human kidney physiology and cancer through the γc signaling pathway. PLoS One. 2012; 7:e31624. [PubMed: 22363690]
70. Lim SP, Leung E, Krissansen GW. The β_7 integrin gene (*Itgb-7*) promoter is responsive to TGF-β1: defining control regions. Immunogenetics. 1998; 48:184–195. [PubMed: 9683663]
71. Reinecker HC, MacDermott RP, Mirau S, Dignass A, Podolsky DK. Intestinal epithelial cells both express and respond to interleukin 15. Gastroenterology. 1996; 111:1706–1713. [PubMed: 8942753]
72. Obermeier F, Hausmann M, Kellermeier S, Kiessling S, Strauch UG, Duitman E, Bulfone-Paus S, Herfarth H, Bock J, Dunger N, et al. IL-15 protects intestinal epithelial cells. Eur J Immunol. 2006; 36:2691–2699. [PubMed: 16981178]

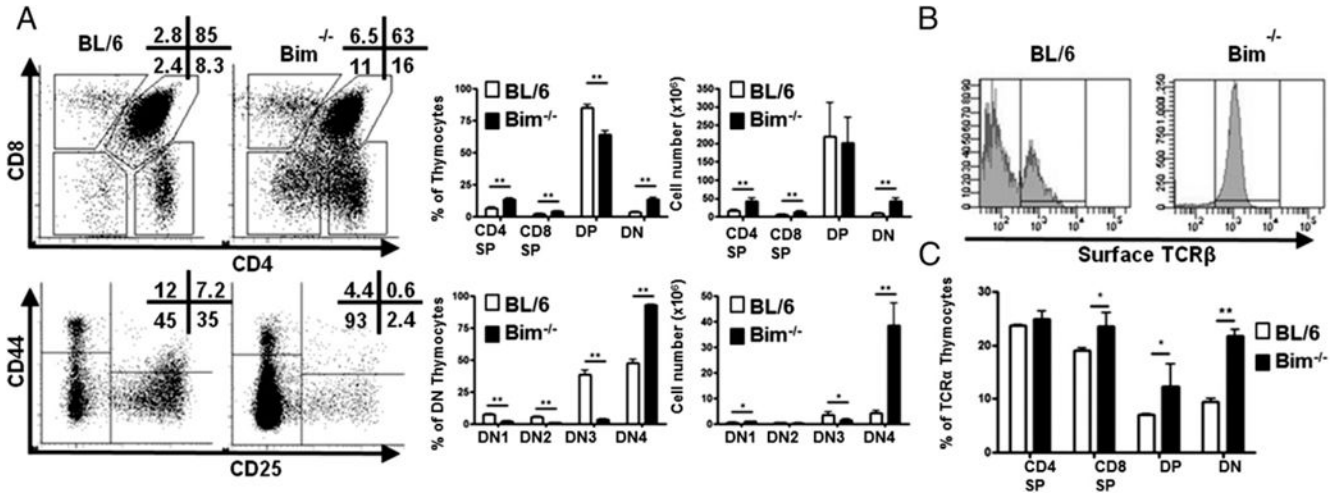

FIGURE 1.

Accumulation of TCR^+ DN thymocytes are observed in the absence of Bim. (**A**) Thymocytes from C57BL/6 (BL/6) or $Bim^{-/-}$ mice ($n = 3$) were stained with Abs and analyzed by flow cytometry. Numbers in representative dot plots show the frequency (percentage) of corresponding populations. The bar graphs show the frequency and cell numbers of each population from either BL/6 (open bars) or $Bim^{-/-}$ (filled bars) mice. (**B**) Histograms show the percentage of $CD25^-CD44^-$ DN thymocytes that express the surface TCRβ-chain. (**C**) Bar graph shows the percentage of $CD25^-CD44^-$ DN thymocytes that express surface TCRα-chain (a combination of Abs against Vα2, Vα3.2, Vα8.3, and Vα11) from either BL/6 (open bars) or $Bim^{-/-}$ (filled bars) mice. Results are representative of at least four independent experiments and show mean ± SD. $*p < 0.05$, $**p < 0.01$. BL/6, C57BL/6.

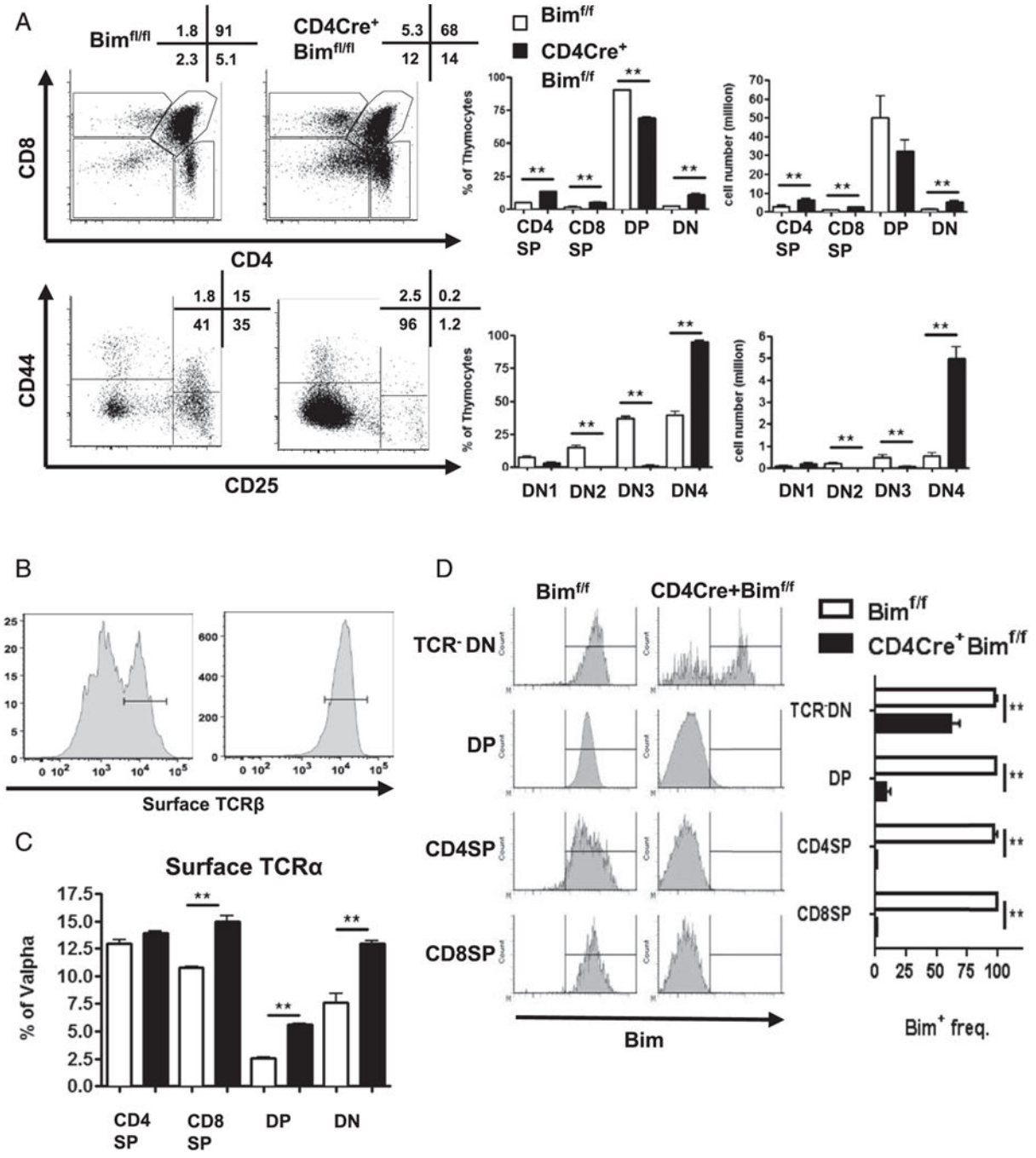

FIGURE 2.

Deletion of Bim at the early DP stage promotes the accrual of TCR^{+} DN thymocytes. (**A**) Thymocytes from Bim$^{f/f}$ or CD4Cre+Bim$^{f/f}$ mice (n = 3) were stained with Abs and analyzed by flow cytometry. Numbers in representative dot plots show the frequency (percentage) of corresponding populations. The bar graphs show the frequency and cell numbers of each population from either Bim$^{f/f}$ (open bars) or CD4Cre^{+}Bim$^{f/f}$ (filled bars) mice. (**B**) Histograms show the percentage of CD25^{-}CD44^{-} DN thymocytes that express surface TCRβ-chain. (**C**) Bar graph shows the percentage of CD25^{-}CD44^{-} DN thymocytes

that express the surface TCRα-chain (a combination of Vα2, Vα3.2, Vα8.3, and Vα11) from either $Bim^{f/f}$ (open bars) or $CD4Cre^{+}Bim^{f/f}$ (filled bars) mice. (**D**) Data in representative histograms show Bim levels in various gated thymic subpopulations, and the bar graphs show the frequency of Bim^{+} cells in thymic subpopulations from either $Bim^{f/f}$ (open bars) or $CD4Cre^{+}Bim^{f/f}$ (filled bars) mice. Results are representative of at least three independent experiments and show mean ± SD. $^{**}p < 0.01$.

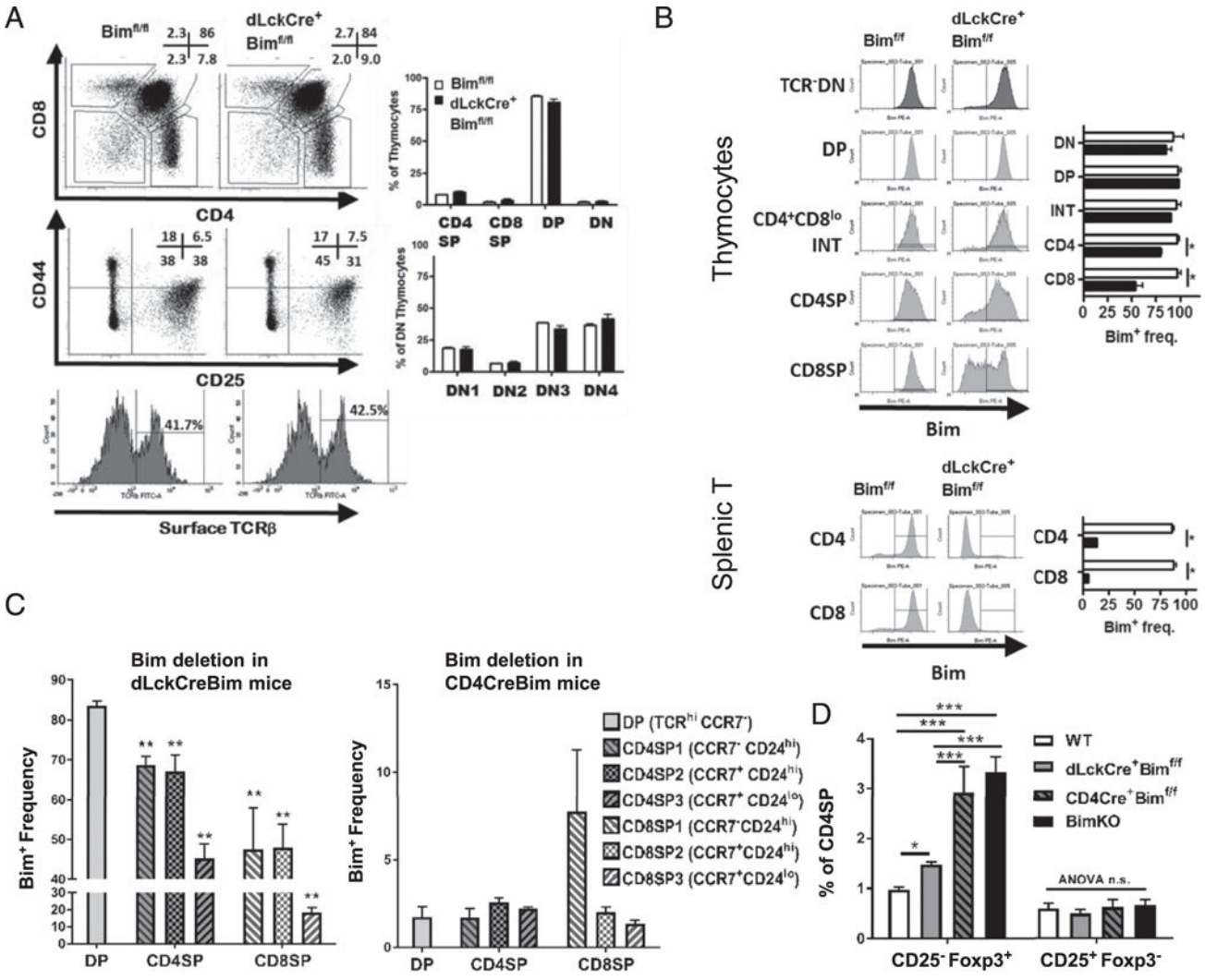

FIGURE 3.

Deletion of Bim at the late DP stage fails to promote TCR$^+$ DN thymocytes. (**A**) Thymocytes from Bim$^{f/f}$ or dLckCre$^+$Bim$^{f/f}$ mice (n = 4) were stained with Abs and analyzed by flow cytometry. Numbers in representative dot plots show the frequency of corresponding populations. Expression of surface TCRβ on CD25$^-$CD44$^-$ DN thymocytes is shown in histograms. The bar graphs show the frequency of each population from either Bim (open bars) or dLckCre$^+$ Bim$^{f/f}$ (filled bars) mice. (**B**) Thymocytes or splenic T cells from Bim$^{f/f}$ or dLckCre$^+$Bim$^{f/f}$ mice were stained with cell surface markers and intracellularly for Bim. Data in representative histograms show Bim levels in various gated thymic subpopulations, and the bar graphs show the frequency of Bim$^+$ cells in thymic subpopulations from either Bim$^{f/f}$ (open bars) or dLckCre$^+$Bim$^{f/f}$ (filled bars) mice. (**C**) The bar graphs show the frequency of Bim$^+$ thymocytes in TCR$^+$CCR7$^-$ DP, SP1 (CCR7$^-$CD24^{hi}), SP2 (CCR7$^+$CD24^{hi}), or SP3 (CCR7$^+$CD24^{1o}) stages from either dLckCre$^+$Bim$^{f/f}$ (left panel) or CD4Cre$^+$Bim$^{f/f}$ (right panel) mice. Statistical comparison was made between each SP subset to DP cells. (**D**) Thymocytes from C57BL/6, dLckCre$^+$Bim$^{f/f}$, CD4Cre$^+$Bim$^{f/f}$, or Bim$^{-/-}$ mice (n = 4–5) were stained with Abs and

analyzed by flow cytometry. The frequencies of thymic Treg precursor populations, $CD25^{-}Foxp3^{+}$ cells, or $CD25^{+}Foxp3^{-}$ cells among CD4SP cells are shown. Results are representative of at least two independent experiments and are shown as mean ± SD. *$p < 0.05$, **$p < 0.01$.

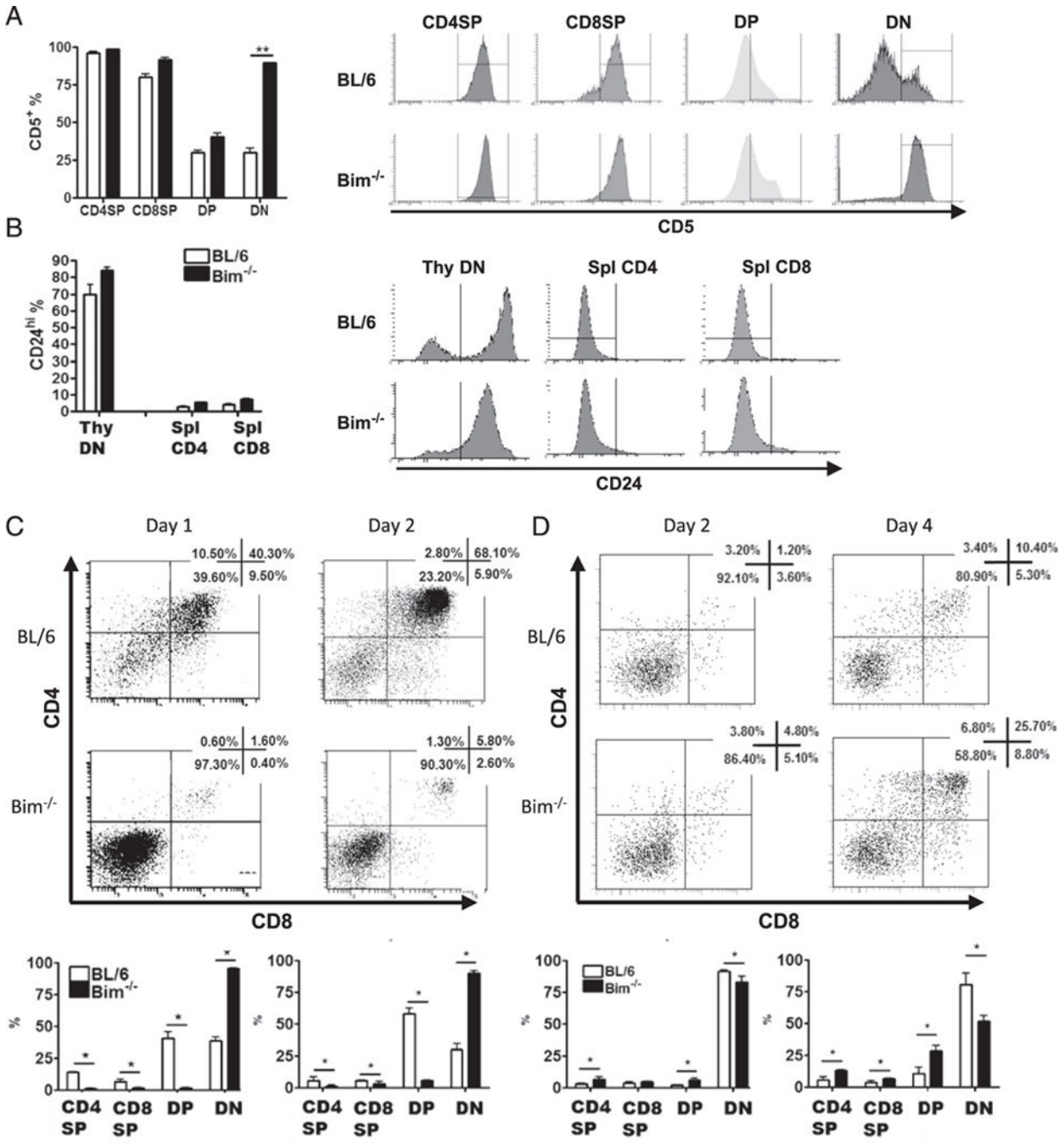

FIGURE 4.

TCR^{+}DN thymocytes in Bim$^{-/-}$ mice express postselection and immature markers and do not develop into DP thymocytes in OP9-DL1 culture. Data show the percentage and histograms of thymocytes or splenic T cells expressing (**A**) the postselection marker CD5 or (**B**) the immature marker CD24, as assessed by flow cytometry. (**C**) Sorted DN4 (CD4^{-}CD8^{-}CD44^{-}CD25^{-}) or (**D**) DN1–3 (CD4^{-}CD8^{-}CD44^{+}CD25^{-}, CD4^{-}CD8^{-}CD44^{+}CD25^{+}, and CD4^{-}CD8^{-}CD44^{-} CD25^{+}) thymocytes from C57BL/6 (BL/6) or Bim$^{-/-}$ mice were cultured with OP9-DL1 cells and IL-7 (1 ng/ml) for indicated

time and analyzed by flow cytometry. Numbers in representative dot plots show the frequency of corresponding populations. The bar graphs show the frequency of each population from either BL/6 (open bars) or $Bim^{-/-}$ (filled bars) mice. Results are representative of at least two independent experiments and show mean ± SD. *$p < 0.05$, **$p < 0.01$. BL/6, C57BL/6.

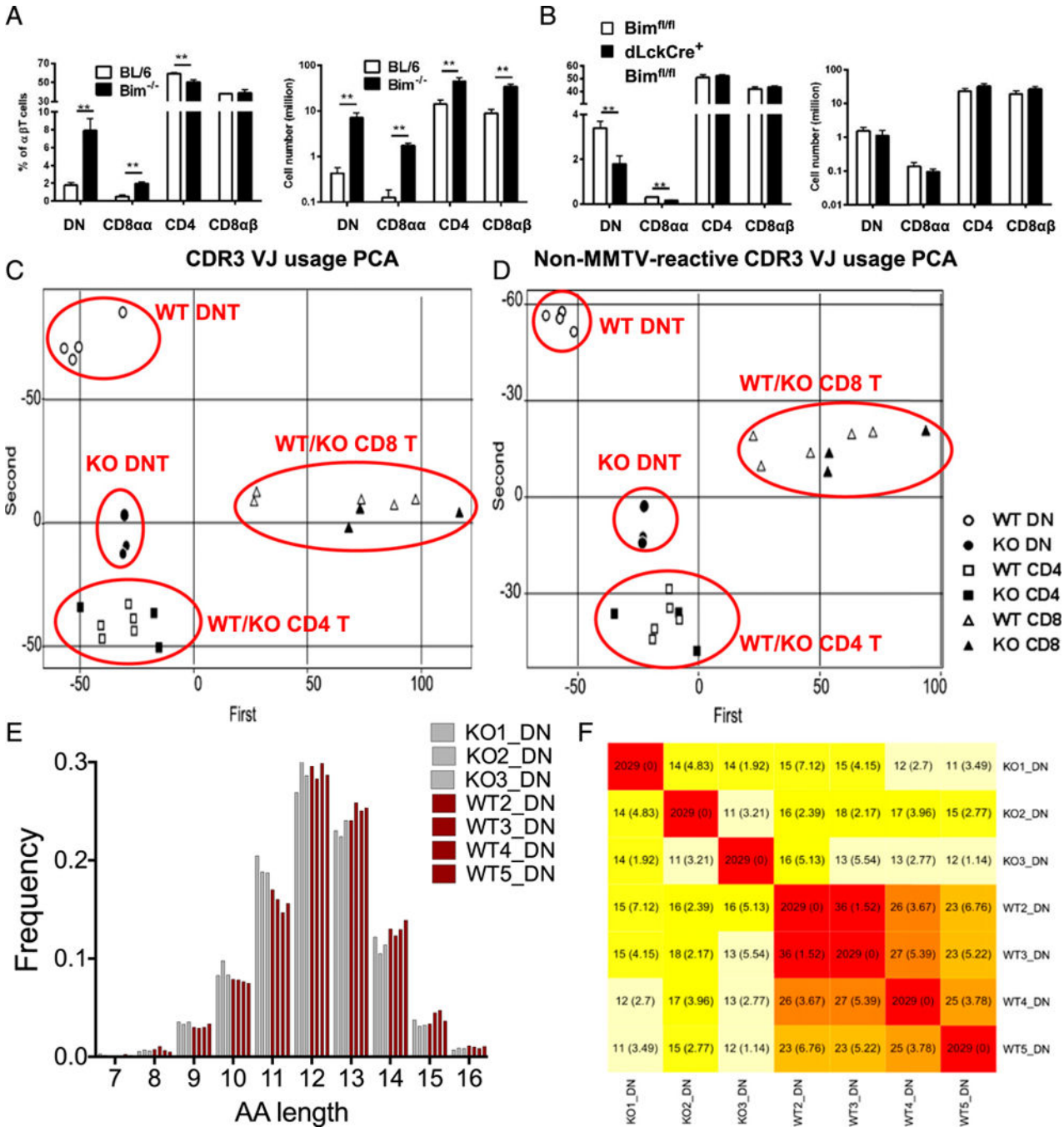

FIGURE 5.

Bim deletion results in DN and CD8αα T cell accumulation in the spleen with distinct TCR repertoire. (**A**) The bar graphs show the percentage of splenic DN ($CD4^{-}CD8\alpha^{-}$), CD8αα ($CD4^{-}CD8\alpha^{+}CD8\beta^{-}$), CD4 ($CD4^{+}CD8\alpha^{-}$), or CD8αβ ($CD4^{-}CD8\alpha^{+}CD8\beta^{+}$) αβT cells ($TCR\beta^{+}$ $CD19^{-}$MHC II^{-} $NK1.1^{-}$), as well as the total cell number, from either C57BL/6 (BL/6; open bars) or $Bim^{-/-}$ (filled bars) mice. (**B**) The bar graphs show the percentage and the total number of splenic DN, CD8αα, CD4, or CD8αβ T cells from $Bim^{f/f}$ (open bars) or $dLckCre^{+}Bim^{f/f}$ (filled bars) mice. Results are representative of at least two independent

experiments ($n \geq 3$ in each group) and show mean ± SD. *$p < 0.05$, **$p < 0.01$. (**C**) Different T cell populations were sorted from an individual BL/6 or $Bim^{-/-}$ mouse, and the TCRβ CDR3 repertoires were sequenced by the Illumina MiSeq system. About 2 million reads were obtained and further normalized and analyzed with MiTCR or tcR software. The scatter plot shows the result of PCA in TCRβ CDR3 V-J chain usage. The clusters of different cell populations are labeled on the plot. (**D**) The scatter plot shows the result of PCA in CDR3 V-J chain usage after removal of mouse mammary tumor virus-reactive TCRβ (TRBV12, TRBV16, and TRBV24) (50, 51). The clusters of different cell populations are labeled on the plot. (**E**) The TCRβ CDR3 lengths (in amino acid [AA] numbers) in DN T cells from either BL/6 (red bars) or $Bim^{-/-}$ (gray bars) mice are plotted. The lengths were analyzed with two-way ANOVA showed significant difference (11 aa, $p < 0.001$; 13 aa, $p < 0.05$). (**F**) The heat map shows the average number (and SD) of public TCRβ CDR3 sequences shared by different mouse among 2029 random subsampled sequences. BL/6, C57BL/6.

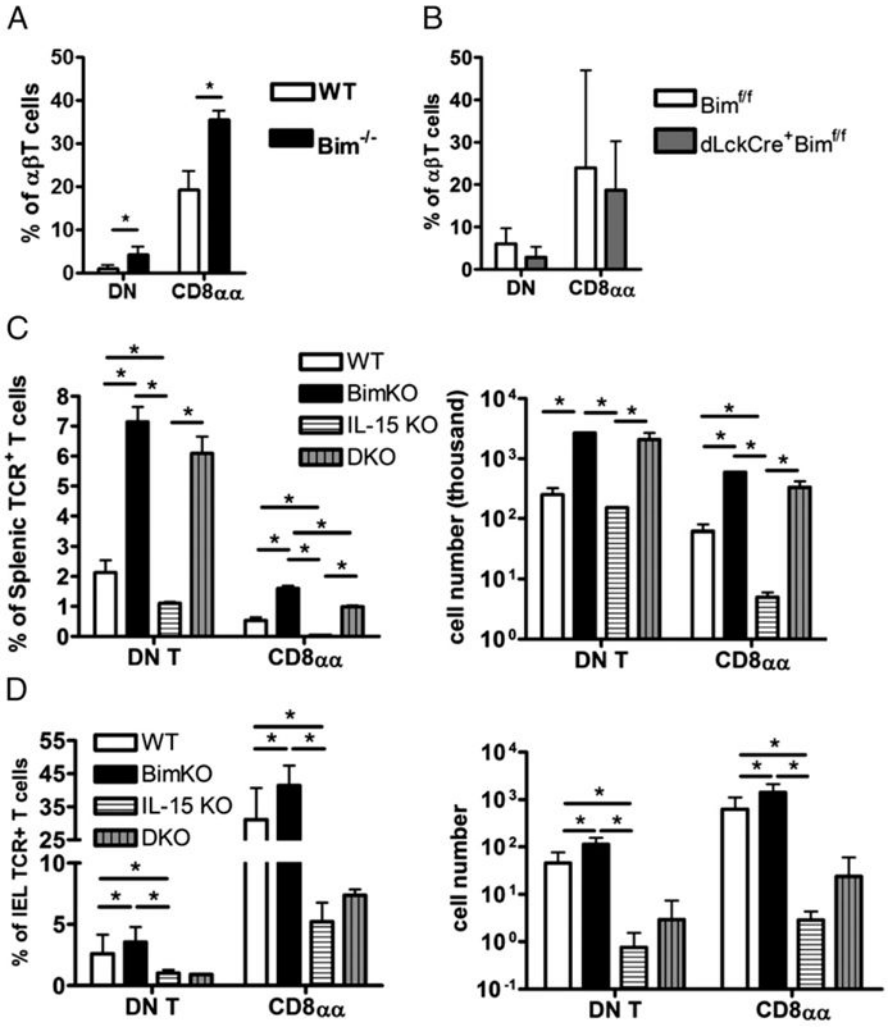

FIGURE 6.

Bim deletion rescues the splenic DN T cells, but not iIELs, in IL-15 knockout (KO) mice. (**A**) The bar graphs show the percentage of small intestinal intraepithelial DN ($CD4^-CD8\alpha^-$) T or CD8αα ($CD4^-CD8\alpha^+$ $CD8\beta^-$) T cell amounts in intraepithelial αβT cells ($TCR\beta^+$ $CD19^-$MHC $II^-NK1.1^-$) from either BL/6 (open bars), $Bim^{-/-}$ (black bars), or (**B**) $dLckCre^+Bim^{f/f}$ (gray bars) mice. (**C**) The bar graphs show the percentage of splenic DN T or CD8αα T cells, as well as the total cell number, from either C57BL/6 (BL/6; open bars), $Bim^{-/-}$ (black bars), IL-15 KO (horizontal-striped bars), or $IL\text{-}15^{-/-}$ Bim (double knockout [DKO], vertical-striped bars) mice. (**D**) The graphs show the percentage and the total number of small intestinal intra-epithelial DN T or CD8αα T cells from either BL/6 (open bars), $Bim^{-/-}$ (black bars), IL-15 KO (horizontal-striped bars), or $IL\text{-}15^{-/-}$ $Bim^{-/-}$ (DKO, vertical-striped bars) mice. Results are representative of at least two independent experiments ($n \geq 3$ in each group) and show mean ± SD. *$p < 0.05$. BL/6, C57BL/6; DKO, double knockout; KO, knockout.

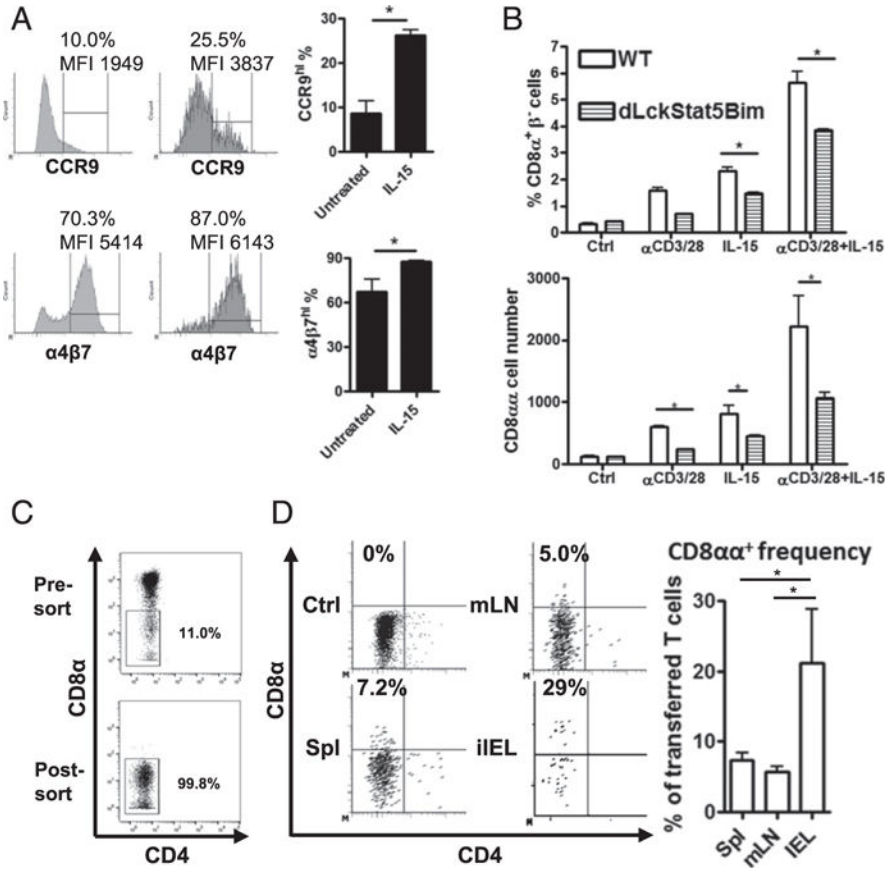

FIGURE 7.

Splenic DN T cells in vitro and in vivo develop into CD8αα T cells, partially depending on IL-15/Stat5 signaling. (**A**) Induction of CCR9 and $\alpha_4\beta_7$ expression in splenic DN T cells. The sorted splenic DN T cells ($CD4^-CD8\alpha^-TCR\beta^+$ $CD19^-$MHC $II^-NK1.1^-$) from $Bim^{-/-}$ mice were cultured with 20 ng/ml rIL-15 for 48 h. The represented histograms of CCR9 or $\alpha_4\beta_7$ expression are shown. The frequency (percentage) and mean fluorescence intensity (MFI) of a $CCR9^{hi}$ or $\alpha_4\beta_7^{hi}$ population are noted on the plots. The bar graphs show the $CCR9^{hi}$ or $\alpha_4\beta_7^{hi}$ percentage within ex vivo splenic DN T cells (untreated) or IL-15–induced CD8αα T cells (IL-15). (**B**) The splenic DN T cells were isolated from either C57BL/6 (BL/6) or $dLckCre^+Bim^{f/f}$ $Stat5^{f/f}$ mice and cultured with plate-bound anti-CD3/CD28 Ab and/or 20 ng/ml rIL-15 for 24 h. The CD8αα T cell frequency and number in the culture were analyzed by flow cytometry. (**C**) The splenic DN T cells ($CD4^-CD8\alpha^-CD19^-NK1.1^-$MHC II^-) were isolated from $Bim^{-/-}$ mice. A represented presort plot and a postsort plot with DN T cell frequency among αβT cells is shown. (**D**) The sorted DN T cells were adoptively transferred into immune-intact BoyJ recipients. After 7 d, T cells in spleen, mesenteric lymph node (mLN), and small intestinal epithelium were analyzed by flow cytometry. The representative dot plots show CD8α and CD4 expression of the donor αβT cells first gated on $CD8\beta^-$ ($CD45.2^+TCR\beta^+CD8\beta^-$), and the frequency represents the CD8αα T cell amounts in donor cells. Results are representative of at least

two independent experiments and show mean ± SD. *$p < 0.05$. BL/6, C57BL/6; MFI, mean fluorescence intensity; mLN, mesenteric lymph node.